

Hybrid Control of the Boost Converter: Robust Global Stabilization

Thomas A.F. Theunisse, Jun Chai, Ricardo G. Sanfelice, and W.P. Maurice H. Heemels

Abstract—In this paper we consider the modeling and (robust) control of a DC-DC boost converter. In particular, we derive a mathematical model consisting of a constrained switched differential inclusion that includes all possible modes of operation of the converter. The obtained model is carefully selected to be amenable for the study of various important robustness properties. By exploiting this model we design a control algorithm that induces robust, global asymptotic stability of a desired output voltage value. The guaranteed robustness properties ensure proper operation of the converter in the presence of spatial regularization to reduce the high rate of switching. The establishment of these properties is enabled by recent tools for the study of robust stability in hybrid systems. Simulations illustrating the main results are included.

I. INTRODUCTION

The increasing number of renewable energy sources and distributed generators requires new strategies for the operation and management of the electricity grid in order to maintain or even to improve the power-supply reliability and quality. Power electronics play a key role in distributed generation and in integration of renewable sources into the electrical grid [1]. A recent challenge for these systems is the unavoidable variability of the power obtained from renewable resources, which, in turn, demands conversion technology that robustly adapts to changes in the supplies and demands.

One type of converter that is widely used in energy conversion is the DC-DC Boost converter. This converter draws power from a DC voltage source and supplies power to a load at a higher DC voltage value. Different approaches have been employed in the literature for the analysis and design of such converters. Arguably, the most popular method used to control such converters is Pulse-Width Modulation (PWM). In PWM-based controllers, the switch in the circuit is turned on at the beginning of each switching period and is turned off when the reference value is lower than a certain carrier signal [2]. In [3], the two steady state configurations of the circuit are averaged, leading to a single differential equation model. More recently, a renewed interest in power converters originated from the rise of switching/hybrid modeling paradigms

[4]–[9], and new perspectives on their control were proposed, including time-based switching, state-event triggered control, and optimization-based control.

In this paper, motivated by the need of converters that robustly adapt to changes in renewable energy systems, we consider the modeling and robust control of a DC-DC boost converter. As a difference to previous models capturing only steady state modes of operation (see, e.g., [4], [5]), inspired by [9], we propose a model that includes all possible modes of operation of the converter. Due to this, we guarantee that both transient behavior and every possible state of the system is captured by the model. Our proposed model for the Boost converter consists of a switching differential inclusion with constraints. Using hybrid systems tools, we study the properties induced by a controller that triggers switches of the differential inclusion based on the value of the internal current and output voltage of the converter as well as on the value of the state of the controller (a logic variable). We formally prove that the controller we employ, which follows the one first proposed in [5] and studied by simulations therein, induces robust, global asymptotic stability of a desired output voltage value. The robustness properties guarantee proper operation of the converter in the presence of spatial regularization to relax the rate of switching. The recently developed tools for robust stability in hybrid systems form the enabling techniques to achieve these important results [10].

The remainder of the paper is organized as follows. After introducing notation, the principles of operation of the Boost converter are discussed and our mathematical model is presented in Section II. A switching control law is presented in Section III. In addition, also in Section III, global asymptotic stability for the closed-loop system is proven. The results on robustness are also presented in Section III. In Section IV, simulations are performed to illustrate our results. Finally, concluding remarks are presented in Section V.

Notation: \mathbb{R}^n denotes n -dimensional Euclidean space, and \mathbb{R} denotes the set of real numbers. $\mathbb{R}_{\geq 0}$ denotes the set of nonnegative real numbers, i.e., $\mathbb{R}_{\geq 0} = [0, \infty)$. \mathbb{N} denotes the set of natural numbers including 0, i.e., $\mathbb{N} = \{0, 1, \dots\}$. \mathbb{B} denotes the closed unit ball in a Euclidean space centered at the origin. Given a set S , ∂S denotes its boundary. Given a vector $x \in \mathbb{R}^n$, $|x|$ denotes the Euclidean vector norm. Given a set $K \subset \mathbb{R}^n$ and a point $x \in \mathbb{R}^n$, the distance of x to the set K is denoted by $|x|_K := \inf_{y \in K} |x - y|$. We use the notation $\overline{\text{co}}$ to denote the closed convex hull of a set. For l vectors $x_i \in \mathbb{R}^{n_i}$, $i = 1, 2, \dots, l$, we denote the vector obtained by stacking all the vectors in one (column) vector $x \in \mathbb{R}^n$ with $n = n_1 + n_2 + \dots + n_l$ by (x_1, x_2, \dots, x_l) ,

T. A. F. Theunisse, and W. P. M. H. Heemels are with the Control Systems Technology group in the Department of Mechanical Engineering, Eindhoven University of Technology, P.O. Box 513, 5600 MB Eindhoven, The Netherlands. Email: t.a.f.theunisse@student.tue.nl, w.p.m.h.heemels@tue.nl. J. Chai, and R. G. Sanfelice are with the Department of Aerospace and Mechanical Engineering, University of Arizona 1130 N. Mountain Ave, AZ 85721. Email: amy89@email.arizona.edu, sricardo@u.arizona.edu. The work of Maurice Heemels was partially supported by the European 7th Framework Network of Excellence Highly-complex and networked control systems (HYCON2) (grant agreement no. 257462). The research by J. Chai and R. G. Sanfelice has been partially supported by the NSF CAREER Grant no. ECS-1150306 and by AFOSR Grant no. FA9550-12-1-0366.

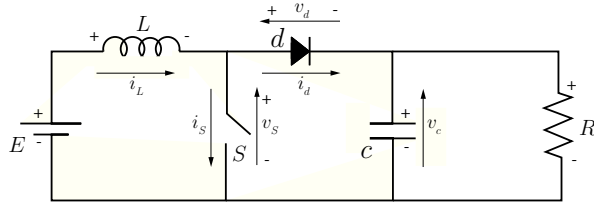


Fig. 1. Schematic representation of a Boost circuit with diode.

i.e., $(x_1, x_2, \dots, x_l) = [x_1^\top, x_2^\top, \dots, x_N^\top]^\top$. A function $\alpha : \mathbb{R}_{\geq 0} \rightarrow \mathbb{R}_{\geq 0}$ is said to be of class \mathcal{K} if it is continuous, zero at zero and strictly increasing. It is said to be of class \mathcal{K}_∞ if it is of class \mathcal{K} and it is unbounded. A function $\beta : \mathbb{R}_{\geq 0} \times \mathbb{R}_{\geq 0} \rightarrow \mathbb{R}_{\geq 0}$ is said to be of class \mathcal{KL} if $\beta(\cdot, t)$ is of class \mathcal{K} for each $t \geq 0$ and $\beta(s, \cdot)$ is nonincreasing and satisfies $\lim_{t \rightarrow \infty} \beta(s, t) = 0$ for each $s \geq 0$.

II. MODELING

In this section we describe the principles of operation of the DC-DC Boost converter. Afterwards, we present a hybrid system model, covering all possible system modes.

A. Principles of Operation

The DC-DC Boost converter is shown in Figure 1. The Boost circuit consists of a capacitor c , an ideal diode d , a DC voltage source E , an inductor L , a resistor R , and an ideal switch S . The voltage across the capacitor is denoted v_c , and the current through the inductor is denoted i_L . The purpose of the circuit is to draw power from the DC voltage source, and supply power to the load at a higher DC voltage value. This task is accomplished by first closing the switch to store energy in the inductor, and then opening the switch to transfer that energy to the capacitor, where it is available to the load.

The presence of switching elements (d and S) causes the overall system to be of a switching/hybrid nature. Depending on the (discrete) state of the diode and of the switch, one can distinguish four modes of operation [9]:

$$\begin{array}{ll} \text{mode 1: } (S = 0, d = 1) & \text{mode 2: } (S = 1, d = 0) \\ \text{mode 3: } (S = 0, d = 0) & \text{mode 4: } (S = 1, d = 1) \end{array}$$

When the system is in mode 1, in which the switch is open ($S = 0$) and the diode is conducting ($d = 1$), the inductor is charged by the input source, which, also offloads power to the resistor. In mode 2, in which the switch is closed ($S = 1$) and the diode is blocking ($d = 0$), the inductor is charged by the input source and the capacitor is offloading its charge to the load. In mode 3, the capacitor offloads its charge to the load. Finally, mode 4, in which the switch is closed, the diode is conducting and the voltage in the capacitor is zero, hence only the inductor is charging.

Using the ideal diode model with two modes, given by $i_d \geq 0, v_d = 0$ (the conducting mode, $d = 1$) and $i_d = 0, v_d \leq 0$ (the blocking mode, $d = 0$), we get four different modes with different S and d combinations. By analyzing the evolution of v_c and i_L for these four modes, we

can derive constrained differential equations for each mode. Conveniently, the equations for mode 2 and mode 4 can be combined into a single mode, which with some abuse of notation, we label as mode 2. Following circuit laws, the constrained differential equations for each mode are given in terms of (v_c, i_L, S) as follows:

$$\begin{array}{l} 1 : \begin{cases} S = 0 \\ \dot{v}_c = -\frac{1}{RC}v_c + \frac{1}{L}i_L \\ \dot{i}_L = -\frac{1}{L}v_c + \frac{E}{L} \\ i_L > 0, \text{ or } (v_c \leq E, i_L = 0) \end{cases} \quad 2 : \begin{cases} S = 1 \\ \dot{v}_c = -\frac{1}{RC}v_c \\ \dot{i}_L = \frac{E}{L} \\ v_c \geq 0 \end{cases} \\ 3 : \begin{cases} S = 0 \\ \dot{v}_c = -\frac{1}{RC}v_c \\ \dot{i}_L = 0 \\ v_c > E, i_L = 0 \end{cases} \end{array}$$

Therefore, the value of the switch S determines whether the system is in mode 1/mode 3 ($S = 0$) or mode 2 ($S = 1$). Note that it is possible that when S changes, v_c and i_L may not be in the regions of viability in the subsequent mode, in which case v_c and i_L should be appropriately reset (e.g., via consistency projectors mapping the state to the algebraic conditions of the subsequent mode [7], [8], [11]). Although, a full model with resets can be derived, see [9], for practical operation of the converter it is clearly undesirable that such resets occur as they may damage the circuit. Therefore our controller will allow $S = 0$ when $i_L \geq 0$, and $S = 1$ only when $v_c \geq 0$. Indeed, in Section III-A, we propose a controller that guarantees that after every switch of S , the algebraic conditions of the subsequent mode are satisfied.

For convenience, we define $x := (v_c, i_L)$ and the algebraic constraints for the modes above in terms of sets as follows:

$$\begin{aligned} M_1 &= \{x \in \mathbb{R}^2 : i_L > 0\} \cup \{x \in \mathbb{R}^2 : v_c \leq E, i_L = 0\}, \\ M_2 &= \{x \in \mathbb{R}^2 : v_c \geq 0\}, \\ M_3 &= \{x \in \mathbb{R}^2 : v_c > E, i_L = 0\} \end{aligned}$$

Hence, $S = 0$ is only allowed when $x \in M_1 \cup M_3$ and $S = 1$ is only allowed when $x \in M_2$. Using these restrictions, we can derive a switched differential inclusion encompassing all the modes of operation derived so far.

B. Mathematical Model

In this section, we define a mathematical model of the Boost converter in which the differential equations in each mode define the continuous dynamics. Since the vector field associated with mode 1 is

$$f_a(x) = \begin{bmatrix} -\frac{1}{RC}v_c + \frac{1}{L}i_L \\ -\frac{1}{L}v_c + \frac{E}{L} \end{bmatrix}$$

and the vector field associated with mode 3 is

$$f_b(x) = \begin{bmatrix} -\frac{1}{RC}v_c \\ 0 \end{bmatrix}$$

the resulting vector field for $S = 0$ is discontinuous. To establish robust asymptotic stability of the upcoming closed-loop system, a Krasovskii regularization of the vector field

will be performed following ideas in [12], [13].¹ The system will take the form of a switched differential inclusion with constraints, namely

$$\dot{x} \in F_S(x) \quad x \in \widetilde{M}_S \quad (1)$$

where $S \in \{0, 1\}$ is the position of the switch S , and for each $S \in \{0, 1\}$, $F_S(x)$ is the Krasovskii regularization of the vector fields and \widetilde{M}_S is the corresponding regularization of the sets capturing the regions of validity for each mode. Solutions will be considered in the sense of Krasovskii [12], [13].

Following [13], the regularization of \widetilde{M}_S for $S = 0$ is $\widetilde{M}_0 = \overline{M}_1 \cup \overline{M}_3 = \{x \in \mathbb{R}^2 : i_L \geq 0\}$, and for $S = 1$ is $\widetilde{M}_1 = \overline{M}_2 = \{x \in \mathbb{R}^2 : v_c \geq 0\}$. Note that for $x \in \overline{M}_3$, f_a and f_b reduce to

$$\begin{aligned} f_a(x)|_{i_L=0} &= \begin{bmatrix} -\frac{1}{Rc}v_c \\ -\frac{1}{L}v_c + \frac{E}{L} \end{bmatrix} \\ f_b(x)|_{i_L=0} &= \begin{bmatrix} -\frac{1}{Rc}v_c \\ 0 \end{bmatrix} \end{aligned}$$

Then, the regularization of the vector field f_0 at each $x \in \widetilde{M}_0$ is given by

$$\begin{aligned} F_0(x) &:= \bigcap_{\delta > 0} \overline{\text{co}} f_0(x + \delta \mathbb{B}) \\ &= \begin{cases} \{f_a(x)\} & \text{if } x \in \overline{M}_1 \setminus \overline{M}_3 \\ \overline{\text{co}} \left\{ \begin{bmatrix} -\frac{1}{Rc}v_c \\ -\frac{1}{L}v_c + \frac{E}{L} \end{bmatrix}, \begin{bmatrix} -\frac{1}{Rc}v_c \\ 0 \end{bmatrix} \right\} & \text{if } x \in \overline{M}_3 \end{cases} \\ &= \begin{cases} \left\{ \begin{bmatrix} -\frac{1}{Rc}v_c + \frac{1}{c}i_L \\ -\frac{1}{L}v_c + \frac{E}{L} \end{bmatrix} \right\} & \text{if } x \in \overline{M}_1 \setminus \overline{M}_3 \\ \left\{ -\frac{1}{Rc}v_c \right\} \times \left[-\frac{1}{L}v_c + \frac{E}{L}, 0 \right] & \text{if } x \in \overline{M}_3 \end{cases} \end{aligned}$$

Since the vector field for mode 2 is given by

$$f_1(x) = \begin{bmatrix} -\frac{1}{Rc}v_c \\ \frac{E}{L} \end{bmatrix}$$

which is continuous, we have, for each $x \in \widetilde{M}_1$, that

$$F_1(x) = \{f_1(x)\} \quad (2)$$

The model (1) is a constrained switched differential inclusion. This is a key difference with previous modeling approaches (see, e.g. [4], [5]) where the third mode is omitted. For this complete model, we propose a controller that induces robust, global asymptotic stability in the next section. As we will see, the hybrid systems approach proposed here is the enabling tool to achieve this result. The model will be used to synthesize a robust globally stabilizing switching control law.

III. A ROBUST GLOBALLY STABILIZING STATE-DEPENDENT SWITCHING CONTROL LAW

In this section, a switching control law for the model of the Boost converter in (1) is proposed. We establish that this control law induces a robust and global asymptotic stability property. Besides that, we determine various robustness properties of the closed-loop system.

¹A Krasovskii regularization of this vector field is used due to the fact that the discontinuity occurs on a set of measure zero. A Filippov regularization would not account for discontinuities on such sets.

A. Control Law

Given a desired set-point voltage $v_c^* > 0$ and current $i_L^* > 0$, let $x^* = (v_c^*, i_L^*)$ and consider the control Lyapunov-function

$$V(x) = (x - x^*)^\top P(x - x^*)$$

where $P = \begin{bmatrix} p_{11} & 0 \\ 0 & p_{22} \end{bmatrix} > 0$. To derive the control law, we compute the inner product between the gradient of V and the directions belonging to the (set-valued) map F_S in (1). By analyzing the inner product of each configuration, for each $S \in \{0, 1\}$ and $x \in \widetilde{M}_S$ we get ,

$$\max_{\xi \in F_S(x)} \langle \nabla V(x), \xi \rangle = \begin{cases} \gamma_0(x) & \text{if } S = 0, x \in \widetilde{M}_0 \\ \gamma_1(x) & \text{if } S = 1, x \in \widetilde{M}_1 \end{cases}$$

where, for each $x \in \mathbb{R}^2$, functions γ_0 and γ_1 are defined as

$$\begin{aligned} \gamma_0(x) &=: 2p_{11}(v_c - v_c^*) \left(-\frac{1}{Rc}v_c + \frac{1}{c}i_L \right) + \\ &\quad 2p_{22}(i_L - i_L^*) \left(\frac{-v_c + E}{L} \right) \\ \gamma_1(x) &=: 2p_{11}(v_c - v_c^*) \left(-\frac{1}{Rc}v_c \right) + 2p_{22}(i_L - i_L^*) \frac{E}{L} \end{aligned}$$

The sign of the functions γ_0, γ_1 will be used to define a state-dependent switching control law assigning the control input S . Let

$$\mathcal{A}_x = \{x \in \mathbb{R}^2 : v_c = v_c^*, i_L = i_L^*\} \quad (3)$$

define the isolated point to be stabilized, namely, the point $(v_c, i_L) = (v_c^*, i_L^*)$. The following lemma establishes a property of functions γ_0, γ_1 that will be used in our stability result in Section III-B.

Lemma 3.1: Let $R, E, p_{11}, p_{22} > 0$, $\frac{p_{11}}{c} = \frac{p_{22}}{L}$, $v_c^* > E$, and $i_L^* = \frac{v_c^{*2}}{RE}$. Then, for each $x \in \mathbb{R}^2 \setminus \mathcal{A}_x$, there exists $S \in \{0, 1\}$ such that

$$\gamma_S(x) < 0 \quad (4)$$

To obtain a control law that does not result in sliding motions and is robust, following the idea in [5], we propose a logic-based control law that selects the input according to the current active input and the value of the state. To this end, let $q \in \{0, 1\}$ be a logic state indicating the value of the actual input S . The controller is defined so that switching of q to $1 - q$ occurs only if $\gamma_q(x)$ becomes zero. Then, when $x \in \mathbb{R}^2 \setminus \mathcal{A}_x$ and $\gamma_q(x) = 0$, by Lemma 3.1, $\gamma_{1-q}(x) < 0$, which makes the closed-loop trajectory components x approach \mathcal{A}_x . The closed-loop system is obtained when S is assigned to q , namely, $S = q$. This leads to the hybrid system \mathcal{H} given by

$$\begin{aligned} \begin{bmatrix} \dot{x} \\ \dot{q} \end{bmatrix} &\in \begin{bmatrix} F_q(x) \\ 0 \end{bmatrix} =: F(x, q) & (x, q) \in C \\ \begin{bmatrix} x^+ \\ q^+ \end{bmatrix} &= \begin{bmatrix} x \\ G_q(x) \end{bmatrix} =: G(x, q) & (x, q) \in D \end{aligned} \quad (5)$$

where

$$\begin{aligned} C &= \left\{ (x, q) : x \in \widetilde{M}_0, \gamma_0(x) \leq 0, q = 0 \right\} \cup \\ &\quad \left\{ (x, q) : x \in \widetilde{M}_1, \gamma_1(x) \leq 0, q = 1 \right\} \end{aligned}$$

$$D = \left\{ (x, q) : x \in \widetilde{M}_0, \gamma_0(x) = 0, q = 0 \right\} \cup \left\{ (x, q) : x \in \widetilde{M}_1, \gamma_1(x) = 0, q = 1 \right\}$$

and

$$G_q(x) = \begin{cases} \{1\} & \text{if } q = 0, \gamma_0(x) = 0 \\ \{0\} & \text{if } q = 1, \gamma_1(x) = 0 \end{cases}$$

The flow map F of the hybrid system \mathcal{H} is constructed by stacking the map F_S (with $S = q$) of (1) and zero, while the flow set enforces the constraints in (1) as well as those of the switching mechanism of the proposed controller. In this way, the continuous evolution of x is according to (1) under the effect of the proposed controller, while q does not change during flows. The jump map G is such that x does not change at jumps and q is toggled at jumps, while the jump set enforces the jumps of the controller within the constraints of (1).

Some sample contour plots and switching boundaries $\gamma_q(x) = 0$ of the proposed controller or a particular set of parameters ($x^* = (7, 3.27)$, $E = 5\text{V}$, $R = 3\Omega$, $c = 0.1\text{F}$, $L = 0.2\text{H}$, $p_{11} = \frac{c}{2}$, $p_{22} = \frac{L}{2}$) are shown in Figure 2.

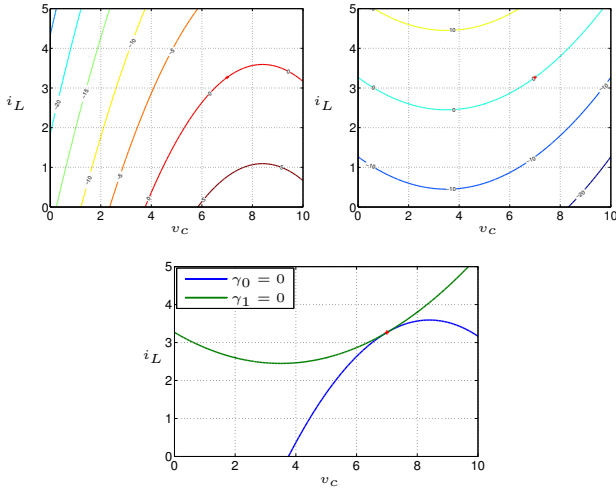


Fig. 2. Contour plots of (upper-left) γ_0 , (upper-right) γ_1 , and (lower) the switching boundaries $\gamma_q(x) = 0$, when $x^* = (7, 3.27)$, $E = 5\text{V}$, $R = 3\Omega$, $c = 0.1\text{F}$, $L = 0.2\text{H}$, $p_{11} = \frac{c}{2}$, and $p_{22} = \frac{L}{2}$.

B. Properties of closed-loop system

Solutions to the closed-loop system \mathcal{H} can evolve continuously and/or discretely depending on flow and jump dynamics. Following [14], we treat the number of jumps as an independent variable j next to the usual time and we parameterize the hybrid time by (t, j) . Solutions to hybrid systems \mathcal{H} are given in terms of hybrid arcs and hybrid inputs on hybrid time domains. Hybrid time domains are subsets E of $\mathbb{R}_{\geq 0} \times \mathbb{N}$ that, for each $(T, J) \in E$, $E \cap ([0, T] \times \{0, 1, \dots, J\})$ can be written as $\cup_{j=0}^{J-1} ([t_j, t_{j+1}], j)$ for some finite sequence of times $0 = t_0 \leq t_1 \leq t_2 \dots \leq t_J$. A hybrid arc ϕ is a function on a hybrid time domain that, for each $j \in \mathbb{N}$, $t \mapsto \phi(t, j)$ is absolutely continuous on the interval $\{t : (t, j) \in \text{dom } \phi\}$. Then, a solution to the

hybrid system \mathcal{H} is given by a hybrid arc ϕ satisfying the dynamics of \mathcal{H} . A solution ϕ to \mathcal{H} is said to be *complete* if $\text{dom } \phi$ is unbounded and *maximal* if there does not exist another pair ϕ' such that ϕ is a truncation of ϕ' to some proper subset of $\text{dom } \phi'$. For more details about solutions to hybrid systems, see [10].

Proposition 3.2: (Properties of solutions) For each $\xi \in C \cup D$, every maximal solution $\chi = (x, q)$ to the hybrid system $\mathcal{H} = (C, F, D, G)$ in (5) with $\chi(0, 0) = \xi$ is complete.

Our goal is to show that the solutions χ to \mathcal{H} in (5) are such that the compact set \mathcal{A} in (3) is asymptotically stable. To this end, we employ the following stability notion for general hybrid systems [10].

Definition 3.3 (Stability): A compact set $\mathcal{A} \subset \mathbb{R}^n$ is said to be

- stable if for each $\varepsilon > 0$ there exists $\delta > 0$ such that each solution χ with $|\chi(0, 0)|_{\mathcal{A}} \leq \delta$ satisfies $|\chi(t, j)|_{\mathcal{A}} \leq \varepsilon$ for all $(t, j) \in \text{dom } \chi$;
- attractive if there exists $\mu > 0$ such that every maximal solution χ with $|\chi(0, 0)|_{\mathcal{A}} \leq \mu$ is complete and satisfies $\lim_{(t, j) \in \text{dom } \chi, t+j \rightarrow \infty} |\chi(t, j)|_{\mathcal{A}} = 0$;
- asymptotically stable if \mathcal{A} is stable and attractive;
- globally asymptotically stable if the attractivity property holds for every point in $C \cup D$.

The following result on the structural properties of \mathcal{H} in (5) is key for robust stability, see [10].

Lemma 3.4: The closed-loop system \mathcal{H} given by (5) satisfies the hybrid basic conditions, i.e., its data (C, F, D, G) is such that²

- (A1) C and D are closed sets;
- (A2) $F : \mathbb{R}^n \rightrightarrows \mathbb{R}^n$ is outer semicontinuous and locally bounded, and $F(x)$ is nonempty and convex for all $x \in C$;
- (A3) $G : \mathbb{R}^n \rightarrow \mathbb{R}^n$ is continuous.

Using these conditions, we are now ready to show the following theorem, which states global asymptotical stability of the compact set \mathcal{A} for the closed-loop system \mathcal{H} .

Theorem 3.5: Consider the hybrid system \mathcal{H} in (5) with $c, L, R, E > 0$. Given a desired set-point voltage and current (v_c^*, i_L^*) , where $v_c^* > E$ and $i_L^* = \frac{v_c^{*2}}{RE}$, then the compact set

$$\mathcal{A} = \mathcal{A}_x \times \{0, 1\} \quad (6)$$

is globally asymptotically stable for \mathcal{H} .

More importantly, since the hybrid closed-loop system in (5) satisfies the hybrid basic conditions (see Lemma 3.4) and the set \mathcal{A} is compact, then, using [10, Theorem 7.21] we have that \mathcal{A} is robustly asymptotically stable. We now

²A set-valued map $S : \mathbb{R}^n \rightrightarrows \mathbb{R}^m$ is *outer semicontinuous* at $x \in \mathbb{R}^n$ if for each sequence $\{x_i\}_{i=1}^{\infty}$ converging to a point $x \in \mathbb{R}^n$ and each sequence $y_i \in S(x_i)$ converging to a point y , it holds that $y \in S(x)$; see [15, Definition 5.4]. Given a set $X \subset \mathbb{R}^n$, it is *outer semicontinuous relative to X* if the set-valued mapping from \mathbb{R}^n to \mathbb{R}^m defined by $S(x)$ for $x \in X$ and \emptyset for $x \notin X$ is outer semicontinuous at each $x \in X$. It is *locally bounded* if, for each compact set $K \subset \mathbb{R}^n$ there exists a compact set $K' \subset \mathbb{R}^n$ such that $S(K) := \cup_{x \in K} S(x) \subset K'$.

have completed the control design and formally established a key closed-loop stability property, in particular, we showed that the basin of attraction is $C \cup D$. It is worth noting that, in addition to pertaining to simpler models (ignoring mode 3) as mentioned before, previous literature lacks the characterization of the basin of attraction.

C. Robustness to spatial regularization

For system (5), we have robustness to general perturbations, but we only present results about spatial regularization here due to space constraints. When the system reaches its desired steady state using the controller in Section III-B, very fast switching may occur. To alleviate this problem, spatial regularization is performed to the closed-loop system \mathcal{H} (at the controller level). More precisely, γ_0 and γ_1 are modified by using a constant factor ρ , with $\rho \in \mathbb{R}_{\geq 0}$. The regularized system will be denoted as \mathcal{H}^ρ , and its flow map is given by the same equation as \mathcal{H} , i.e.,

$$\begin{bmatrix} \dot{x} \\ \dot{q} \end{bmatrix} \in \begin{bmatrix} F_q(x) \\ 0 \end{bmatrix} \quad (x, q) \in C_\rho,$$

where, now, the flow set is replaced by

$$C_\rho = \left\{ (x, q) : x \in \widetilde{M}_0, \gamma_0(x) \leq \rho, q = 0 \right\} \cup \left\{ (x, q) : x \in \widetilde{M}_1, \gamma_1(x) \leq \rho, q = 1 \right\}$$

Furthermore, the jump map is given by

$$\begin{aligned} x^+ &= x \\ q^+ &\in G_q(x) \end{aligned} \quad (x, q) \in D_\rho,$$

where, now, the jump set is replaced by

$$D_\rho = \left\{ (x, q) : x \in \widetilde{M}_0, \gamma_0(x) = \rho, q = 0 \right\} \cup \left\{ (x, q) : x \in \widetilde{M}_1, \gamma_1(x) = \rho, q = 1 \right\}$$

and

$$G_q(x) = \begin{cases} \{1\} & \text{if } q = 0, \gamma_0(x) \geq \rho \\ \{0\} & \text{if } q = 1, \gamma_1(x) \geq \rho \end{cases}$$

The new switching boundaries for a particular set of parameters ($x^* = (7, 3.27)$, $E = 5\text{V}$, $R = 3\Omega$, $c = 0.1\text{F}$, $L = 0.2\text{H}$, $p_{11} = \frac{c}{2}$, $p_{22} = \frac{L}{2}$, and $\rho = 2$) are shown in Figure 3.

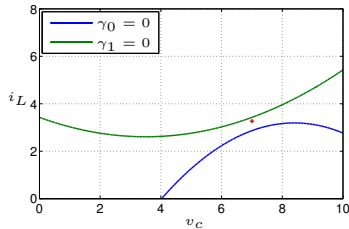


Fig. 3. Switching boundaries with spatial regularization where $\rho = 2$, using ($x^* = (7, 3.27)$, $E = 5\text{V}$, $R = 3\Omega$, $c = 0.1\text{F}$, $L = 0.2\text{H}$, $p_{11} = \frac{c}{2}$, and $p_{22} = \frac{L}{2}$).

Theorem 3.6: *Under the assumptions of Theorem 3.5, there exists $\beta \in \mathcal{KL}$ such that, for each $\varepsilon > 0$ and each*

compact set $K \subset \mathbb{R}^2$, there exists $\rho^ > 0$ guaranteeing the following property: for each $\rho \in (0, \rho^*]$ every solution $\chi = (x, q)$ to \mathcal{H}^ρ with $\chi(0, 0) \in K \times \{0, 1\}$ is such that its x component satisfies*

$$|x(t, j)|_{\mathcal{A}_x} \leq \beta(|x(0, 0)|_{\mathcal{A}_x}, t+j) + \varepsilon \quad \forall (t, j) \in \text{dom } \chi. \quad (7)$$

The property asserted by Theorem 3.6 will be illustrated numerically in Section IV-B.

IV. SIMULATION RESULTS

In this section, we present several simulation results. First, the closed-loop system \mathcal{H} is simulated for the ideal case. Due to undesirable chattering, the spatial regularized system \mathcal{H}^ρ is simulated next. The simulations are performed using $E = 5\text{V}$, $R = 3\Omega$, $c = 0.1\text{F}$, $L = 0.2\text{H}$, and $P = \begin{bmatrix} \frac{c}{2} & 0 \\ 0 & \frac{L}{2} \end{bmatrix}$, unless noted otherwise, within the HYBRID EQUATIONS TOOLBOX [16].

A. Simulating the closed-loop system

The results for initial conditions $x_0 = (0, 5)$ and $x_0 = (5, 0)$ for the closed-loop system \mathcal{H} are shown in Figure 4. As can be seen, the solutions converge from both initial conditions to the set \mathcal{A} .

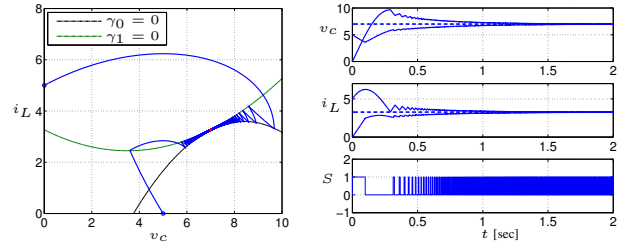


Fig. 4. Simulation results for the closed loop system \mathcal{H} with initial conditions $x_0 = (0, 5)$, $q_0 = 1$ and $x_0 = (5, 0)$, $q_0 = 0$, and where S is only drawn for the simulation using $x_0 = (5, 0)$.

Though not formally established in this paper, the closed-loop system is robust to slowly varying parameters. To illustrate this, a simulation is performed with a dynamically changing set point x^* . Initially, $x^* = (7, 3.27)$, but when a neighborhood of this value is reached, we linearly increase x^* from $(7, 3.27)$ to $(10, 6.67)$. This simulation is shown in Figure 5. As it can be seen, the Boost converter follows the reference well and eventually reaches a neighborhood of the final x^* .

B. Simulating the spatially regularized closed-loop system

Now, the spatially regularized closed-loop system \mathcal{H}^ρ is implemented. The results for initial conditions $x_0 = (0, 5)$, $q_0 = 1$ and $x_0 = (5, 0)$, $q_0 = 0$ are shown in Figure 6.

To validate Theorem 3.6, more simulations are performed in order to find a relationship between the spatially regularization parameter ρ and ε in Theorem 3.6. From the simulation results shown in Table I, the relationship between ρ and ε , specifically, for $x^* = (7, 3.27)$, can now be approximated as

$$\varepsilon \approx 0.9\rho \quad (8)$$

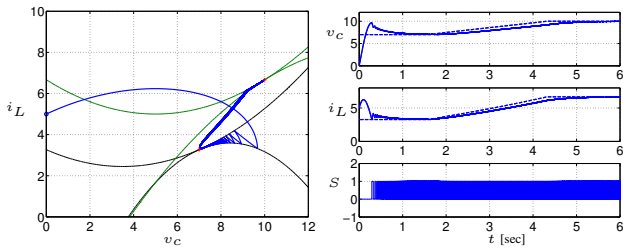


Fig. 5. Simulation results with initial conditions $x_0 = (0, 5)$, $q_0 = 0$, when x^* linearly changes from $(7, 3.27)$ to $(10, 6.67)$, where the black and green curves denote the switching boundaries for $x^* = (7, 3.27)$ and $x^* = (10, 6.67)$, respectively.

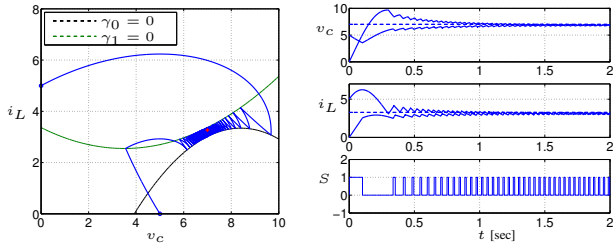


Fig. 6. Simulation results for the spatially regularized closed loop system \mathcal{H}^ρ with $\rho = 0.5$ for initial conditions $x_0 = (0, 5)$, $q_0 = 1$ and $x_0 = (5, 0)$, $q_0 = 0$, and where S is only drawn for the simulation using $x_0 = (5, 0)$.

TABLE I

SIMULATION RESULTS FOR DIFFERENT VALUES OF ρ .

ρ	$\lim_{t+j \rightarrow \infty} \overline{v_c}(t, j)$	$\lim_{t+j \rightarrow \infty} \overline{i_L}(t, j)$	ε	ε/ρ
0.01	6.993	3.261	0.0090	0.90
0.05	6.974	3.241	0.0365	0.73
0.1	6.944	3.211	0.0790	0.79
0.5	6.719	2.991	0.3936	0.78
1	6.422	2.707	0.8046	0.80
2	5.721	2.072	1.7502	0.88

As it can be seen, the larger the spatial regularization (larger ρ) the larger the error will be. Eventually, when ρ becomes too large, the controller may not be able to stabilize the desired point x^* .

V. CONCLUSIONS

In this paper, a hybrid system approach for control of the Boost converter is presented. First of all, a switched system with discontinuous right-hand side for all the modes is obtained. For this model, a suitable Krasovskii regularization is determined, leading to a switched differential inclusion with constraints, after which a control design procedure is proposed. By formalizing the whole control setup in the hybrid systems framework of [10] and establishing important basic properties of the control scheme, various important stabilization and robustness properties can be derived, in particular robust global stability of a set point (v_c^*, i_L^*) . To the best of our knowledge, no such a characterization was published before for this circuit. Using the proposed control law, we showed how to systematically deal with spatial regularization to reduce the switching rate of the converter. Multiple simulations are performed to illustrate the different

properties (e.g., stability, and robustness properties) of the closed-loop system.

REFERENCES

- [1] J.M. Carrasco, L. G. Franquelo, J. T. Bialasiewicz, E. Galvan, R. C. P. Guisado, Ma. A. M. Prats, J. I. Leon, and N. Moreno-Alfonso. Power-electronic systems for the grid integration of renewable energy sources: A survey. *IEEE Transactions on Industrial Electronics*, 53:1002–1016, 2006.
- [2] F. Vasca and L. Iannelli. *Dynamics and Control of Switched Electronic Systems*. Springer-Verlag, 2012.
- [3] R. D. Middlebrook and S. Cuk. A general unified approach to modelling switching-converter power stages. In *Power Electronics Specialists Conference*, pages 18–34, 1976.
- [4] M. Senesky, G. Eirea, and T.J. Koo. Hybrid modelling and control of power electronics. In Oded Maler and Amir Pnueli, editors, *Hybrid Systems: Computation and Control*, volume 2623 of *Lecture Notes in Computer Science*, pages 450–465. Springer Berlin Heidelberg, 2003.
- [5] J. Buisson, P.Y. Richard, and H. Cormerais. On the stabilisation of switching electrical power converters. In Manfred Morari and Lothar Thiele, editors, *Hybrid Systems: Computation and Control*, volume 3414 of *Lecture Notes in Computer Science*, pages 184–197. Springer Berlin Heidelberg, 2005.
- [6] T. Geyer, G. Papafotiou, and M. Morari. On the optimal control of switch-mode dc-dc converters. In Rajeev Alur and George J. Pappas, editors, *Hybrid Systems: Computation and Control*, volume 2993 of *Lecture Notes in Computer Science*, pages 342–356. Springer Berlin Heidelberg, 2004.
- [7] M.K. Camlibel, W.P.M.H. Heemels, A.J. Van Der Schaft, and J.M. Schumacher. Switched networks and complementarity. *Circuits and Systems I: Fundamental Theory and Applications, IEEE Transactions on*, 50(8):1036–1046, 2003.
- [8] W.P.M.H. Heemels, M.K. Camlibel, A.J. Van Der Schaft, and J.M. Schumacher. On the dynamic analysis of piecewise linear networks. *Circuits and Systems I: Fundamental Theory and Applications, IEEE Transactions on*, 49(3):315–327, 2002.
- [9] W.P.M.H. Heemels, M.K. Camlibel, A.J. Schaft, and J.M. Schumacher. Modelling, well-posedness, and stability of switched electrical networks. In Oded Maler and Amir Pnueli, editors, *Hybrid Systems: Computation and Control*, volume 2623 of *Lecture Notes in Computer Science*, pages 249–266. Springer Berlin Heidelberg, 2003.
- [10] R. Goebel, R. G. Sanfelice, and A. R. Teel. *Hybrid Dynamical Systems: Modeling, Stability, and Robustness*. Princeton University Press, New Jersey, 2012.
- [11] D. E. Schwarz. *Consistent initialization for index-2 differential algebraic equations and its application to circuit simulation*. PhD thesis, 2000.
- [12] N.N. Krasovskii and A.I. Subbotin. *Game-Theoretical Control Problems*. Springer-Verlag, 1988.
- [13] R.G. Sanfelice, R. Goebel, and A.R. Teel. Generalized solutions to hybrid dynamical systems. *ESAIM: Control, Optimisation and Calculus of Variations*, 14(4):699–724, 2008.
- [14] R. G. Sanfelice and C. Prieur. Uniting two output-feedback hybrid controllers with different objectives. In *Proc. 29th American Control Conference*, pages 910–915, 2010.
- [15] R.T. Rockafellar and R. J-B Wets. *Variational Analysis*. Springer, Berlin Heidelberg, 1998.
- [16] R. G. Sanfelice, D. A. Copp, and P. Nãñez. A toolbox for simulation of hybrid systems in Matlab/Simulink: Hybrid Equations (HyEQ) Toolbox. *Proceedings of Hybrid Systems: Computation and Control Conference*, 101–106, 2013.